



HHS Public Access

Author manuscript

Expert Opin Drug Deliv. Author manuscript; available in PMC 2024 July 15.

Published in final edited form as:

Expert Opin Drug Deliv. 2021 March ; 18(3): 383–398. doi:10.1080/17425247.2021.1835858.

Drug-eluting embolic microspheres: State-of-the-art and emerging clinical applications

Andrew S. Mikhail¹, Ayele H. Negussie¹, Michal Mauda-Havakuk¹, Joshua W. Owen¹, William F. Pritchard¹, Andrew L. Lewis², Bradford J. Wood^{1,*}

¹Center for Interventional Oncology, Radiology and Imaging Sciences, Clinical Center, National Institutes of Health, Bethesda, Maryland, USA 20892

²Biocompatibles UK, Ltd. (now Boston Scientific Corp.), Lakeview, Riverside Way, Watchmoor Park, Camberley, GU15 3YL, UK

Abstract

Introduction: Drug-eluting embolic (DEE) microspheres, or drug-eluting beads (DEB), delivered by transarterial chemoembolization (TACE) serve as a therapeutic embolic to stop blood flow to tumors and a drug delivery vehicle. New combinations of drugs and DEE microspheres may exploit potential synergy between mechanisms of drug activity and local tissue responses generated by TACE to enhance the efficacy of this mainstay therapy.

Areas covered: This review provides an overview of key drug delivery concepts related to DEE microspheres with a focus on recent technological developments and promising emerging clinical applications as well as speculation into the future.

Expert opinion: TACE has been performed for nearly four decades by injecting chemotherapy drugs into the arterial supply of tumors while simultaneously cutting off their blood supply, trying to starve and kill cancer cells, with varying degrees of success. The practice has evolved over the decades but has yet to fulfill the promise of truly personalized therapies envisioned through rational selection of drugs and real-time multi-parametric image guidance to target tumor clonality or heterogeneity. Recent technologic and pharmacologic developments have opened the door for potentially groundbreaking advances in how TACE with DEE microspheres is performed with the goal of achieving advancements that benefit patients.

* **Correspondence:** Bradford J. Wood, Phone: +1 301 496 773, bwood@nih.gov.

Declaration of interest

BJ Wood and NIH have intellectual property in the space. Patents on imageable beads and imageable drug-eluting bead technologies include patent #US10307493 Imageable Embolic Microsphere, PCT WO 2014/152488 Imageable Embolic Microsphere, Japan JP6420817 Imageable embolic microspheres, and Bismuth image-able drug eluting microsphere for chemoembolization. The NIH has a Cooperative Research and Development Agreement with each of the following: Philips Research, Biocompatibles UK Ltd / BTG now Boston Scientific Corporation, Celsion Corp, and Siemens Healthineers. BJ Wood is the Principle Investigator for these research agreements. WF Pritchard, AS Mikhail, M Mauda-Havakuk, AH Negussie, and JW Owen participate in the related research. AL Lewis was previously VP of R&D for BTG (now Boston Scientific) and is currently Director for R&D at OwenMumford Ltd. The content of this manuscript does not necessarily reflect the views or policies of the U.S. Department of Health and Human Services. The mention of commercial products, their source, or their use in connection with material reported herein is not to be construed as an actual or implied endorsement of such products by the United States government.

Keywords

microsphere; bead; embolization; TACE; DEB; chemoembolization; drug delivery; doxorubicin; hepatocellular carcinoma; embolic

1. Introduction

Liver cancer is a leading cause of cancer-related death worldwide and has continued to increase in incidence and mortality for several decades [1]. Hepatocellular carcinoma (HCC), the predominant form of liver cancer, is usually diagnosed at advanced stages of tumor development when transplantation, surgical resection, or local thermal ablation may not be feasible. For many of these patients, minimally invasive regional therapy with transarterial chemoembolization (TACE) may be a palliative option.

TACE is the recommended first-line therapy for patients with intermediate-stage HCC [2] and it has also been used to treat patients with hepatic metastasis from primary gastrointestinal, breast, melanoma, and neuroendocrine tumors [3–6]. The procedure is performed by delivering chemotherapy and embolic materials directly into tumor-supplying arteries under imaging guidance. The rationale for TACE is that selective disruption of blood flow to hepatic arteries parasitized by tumors and concomitant delivery of chemotherapy results in tumor-localized ischemic and cytotoxic effects. For conventional TACE (cTACE), a chemotherapeutic drug is emulsified in ethiodized oil (Lipiodol®) and administered transarterially followed by an embolic. More recently, TACE has also been performed with drug-eluting embolic (DEE) microspheres, also referred to as drug-eluting beads (DEB), that serve both as an embolic and locoregional drug delivery vehicle. TACE with DEE microspheres results in greater drug concentrations in tumors and reduced systemic drug exposure compared to intra-arterial infusions of free drug [7, 8] or cTACE [9, 10].

Despite its widespread adoption, there remains little agreement on treatment parameters including the type and size of embolic, drug selection, catheter selectivity for tumor arteries, or definition of treatment endpoints. This has contributed to substantial variability in local operator practices and procedural techniques at the expense of reproducibility and comparability. In addition, there is a lack of understanding regarding the relative contribution of the drug *versus* the embolic towards treatment efficacy. Indeed, results comparing the outcomes of embolization using bland microspheres (no drug) to embolization using DEE microspheres loaded with doxorubicin, a chemotherapeutic drug, have been mixed and there remains no consensus regarding which approach is superior. This has spurred investigations into drugs with various different modes of action with the goal of better exploiting potential synergy between mechanisms of drug activity and local tissue responses generated by TACE.

The ideal drug candidate for delivery with DEE microspheres should load into the microspheres in high concentrations, have a sustained or tunable drug release profile, and penetrate readily into surrounding tissue. Moreover, its activity should be maintained or enhanced within the post-TACE tumor microenvironment and counteract or promote biologic processes stimulated by embolization. For example, antiangiogenic drugs eluted

from DEE microspheres may help to counteract neoangiogenic pathways stimulated by TACE-induced tissue hypoxia that can promote tumor recurrence. With the development of immunotherapy, combinations of DEE microspheres and immune-modulating agents could provide potent local, and potentially systemic, therapeutic effects by promoting antitumor immune responses within the inflammatory microenvironment created by TACE, or by helping to overcome pathways of immune resistance or tolerance.

Novel DEE platforms are also under development which may complement or provide new capabilities for TACE and enhance drug delivery and efficacy. Recently, DEE microspheres that are visible on intra-procedural fluoroscopy and cone beam CT (CBCT) imaging have been developed [11–14] raising the intriguing possibility that microsphere radiopacity could serve as a surrogate for spatial drug levels, enabling spatial drug dosimetry [15]. DEE microspheres containing a variety of radiopacifiers have been developed that could potentially enable differentiation on CT imaging between microspheres loaded with different drugs enabling rational delivery of specific drugs to discrete microenvironments within the tumor [16, 17].

The goal of this review is to highlight recent advances in DEE microsphere-based drug delivery, and to explore emerging and yet-to-be-explored strategies to improve the efficacy of TACE with DEE microspheres.

2. Tumor-localized drug delivery using DEE microspheres

The concept of using microspheres to enhance drug delivery to the liver dates back several decades [18, 19] and is based on the original idea that temporary or permanent occlusion of hepatic blood flow following intra-arterial drug infusion can increase drug retention in tumors, reduce washout, and limit systemic exposure, potentially reducing side effects and enhancing efficacy. Drug-eluting microspheres combine both embolic and drug delivery mechanisms into a single vector, with the delivered drug initially co-localized with the embolic microspheres.

The safety, efficacy, and pharmacokinetics of DEE microspheres loaded with doxorubicin were demonstrated by landmark clinical trials reported in 2007 and 2010 which showed significant reductions in peak plasma drug concentrations and area under the curve, as well as increased objective response in patients with advanced HCC, compared to cTACE [9, 10, 20]. In this section, we provide an overview of DEE microspheres developed using permanent or biodegradable materials with the capacity to entrap and release drug in a controlled manner.

2.1 Commercially available DEE microspheres

Currently there are six commercial DEE microspheres with CE marking: five non-degradable and one biodegradable (Table 1). Initial clinical experience with an additional DEE microsphere, Callispheres, has been reported [21–23]. No microspheres have been approved by the U.S. Food and Drug Administration for marketing as DEE devices therefore their use is investigational or off-label when drug-loaded. The microspheres' chemical compositions and physical characteristics are summarized in Table 1.

Differences in chemical structures among these microspheres impart different drug loading capacities and rates of drug release [44], parameters that directly impact *in vivo* pharmacokinetics. Differences in size, size range and dispersity, and mechanical properties, e.g., compressibility and deformability, may influence the *in vivo* performance of microspheres including their distribution and packing density in arteries, ischemic effects, and treatment-specific toxicity. These properties can also affect microsphere handling characteristics and compatibility with micro-catheters. Clinical investigations of DEE microspheres should be performed in compliance with applicable regulations after consultation with appropriate regulatory bodies.

2.2 Drug loading and release

All of the currently marketed DEE microspheres are loaded at the point of use (normally in the hospital pharmacy) by mixing with a drug solution followed by occasional shaking. The time needed for drug loading is dependent upon drug concentration and type, as well as the size, quantity, and type of microspheres [48–50]. Drug loading occurs via an active uptake mechanism driven by the ionic interaction between cationic drugs, usually containing one or more protonated amine groups, and negatively charged sulfonate (SO_3^-) or carboxylate (COO^-) moieties within the microsphere polymer structure [44, 48, 51]. Formation of drug salts in acidic solution can improve drug solubility and promote loading into the microspheres by providing one or more positive charges for interaction with the anionic moieties of the microspheres.

Drug release occurs by ion-exchange whereby the drug is displaced by positively charged ions in the elution media, blood or tissues. The rate of drug release is a function of one or more factors including the strength of the ionic interactions between drug and microspheres, drug-drug interactions within the microspheres (as in the case of doxorubicin) and the ionic strength of the elution medium [52–54]. As a result, under the same conditions, different drugs have different relative rates of release from microspheres ranging from water soluble drugs with little or no interaction with the microspheres that release quickly, to those with moderate (e.g. irinotecan), and relatively slow (e.g. doxorubicin) release rates [55]. Drugs with chemical structures that promote molecular aggregation within the microspheres may prolong drug elution [53, 56]. In addition, smaller microspheres tend to have faster elution rates due to their higher surface area to volume ratio relative to larger microspheres [53]. Drug solubility and concentration in the elution medium can also influence the rate of drug release and diffusion from the microspheres [53].

In vitro drug elution studies are normally conducted using techniques for dissolution testing described in the US pharmacopeia (Chapter <711>) [57]. However, no single technique can accurately predict drug release kinetics *in vivo*. Instead, *in vitro* elution studies provide a means for comparing relative release rates among drugs under controlled conditions and may provide an indication of the relative extent of systemic exposure *in vivo*.

One limitation of current commercially available DEE microspheres is that, in their native form, they can only load and release positively charged drugs due to the anionic nature of their polymer matrices. Other DEE microspheres with different physicochemical properties and drug delivery mechanisms may load and release other varieties of drugs [58]. Some

drugs that cannot be actively loaded into DEE microspheres may be incorporated into the microspheres using solvents or by precipitating poorly water-soluble drugs into the microsphere matrix [59, 60].

Although there is no currently approved DEE microsphere available in which the drug is pre-loaded into the microsphere matrix, a number of clinical studies have used this product format [10, 61–63]. In these studies, doxorubicin, irinotecan, or vandetanib was loaded into the microspheres by the manufacturer and lyophilized in order to produce a sterile vial of dry microspheres that were hydrated with water at the point of use. This approach has the advantage of eliminating preparation time normally needed for drug loading, providing rapid intraprocedural access to drug-loaded microspheres.

2.3 Biocompatibility and safety

Commercial DEE microspheres are required to undergo biocompatibility evaluations in order to demonstrate that the unloaded microsphere matrix has no long-term adverse effects. This may include various tests for cytotoxicity of leachable chemicals as well as short-, medium- and long-term studies of local effects including tissue reactions following DEE microsphere delivery in animals [34, 64–66].

TACE with DEE microspheres for treatment of HCC tumors is a safe procedure with reported rates of serious adverse events ranging from 6.7 to 20.4% [10, 20, 67, 68]. Post embolization syndrome following TACE with DEE microspheres, as also seen with cTACE or embolization with bland microspheres, consisting of abdominal pain, fever, nausea and vomiting has been reported in 24.7–84% of patients but is self-limiting [10, 20, 68, 69]. Transient elevations in liver enzymes including aspartate aminotransferase, alanine aminotransferase, and bilirubin are known to occur in humans [70] and animal models [71–73]. Lower rates of chemotherapy-related adverse events have been reported for TACE with doxorubicin-loaded DEE microspheres compared to cTACE and is likely attributable to lower systemic levels of doxorubicin [20].

2.4 Biodegradable DEE microspheres

The rationale for biodegradable (resorbable) DEE microspheres is that they may be used for temporary occlusion of blood vessels to permit repeat procedures or in an effort to limit the duration of tissue hypoxia which has been implicated in the stimulation of neoangiogenesis. Biodegradable DEE microspheres have been developed using natural [74–77] or synthetic [78–81] materials that degrade primarily by hydrolysis. However, depending on local hemodynamic and coagulative conditions, it is possible for biodegradable embolics (or any embolic) to cause permanent vessel occlusion if a thrombus or vessel damage persists despite microsphere degradation. Overall, the potential benefits of biodegradable DEE microspheres remain speculative.

There are a number of potentially important characteristics that should be considered when designing biodegradable DEE microspheres. For example, the microspheres should degrade into small soluble components, avoiding potential dislodgement of large fragments that could lead to non-target embolization or inflammation. In addition, drug release should occur in a controlled manner governed by or within the timeframe of microsphere

degradation. Similarly, microspheres should degrade at a desirable rate so as to balance the duration of tissue ischemia with desired vessel recanalization.

One example of a synthetic resorbable DEE microsphere was developed from poly(ethylene glycol) methacrylate (PEGMA) crosslinked with a hydrolyzable copolymer consisting of poly(lactide-co-glycolide) (PLGA) and poly(ethylene glycol) (PEG) (PLGA-PEG-PLGA) [82, 83]. To shorten the size of the polymer degradation products, additional hydrolyzable ester linkages were incorporated into the hydrogel matrix using 2-methylene-1,3-dioxepane [82, 83]. The proposed benefit of this approach is that small, water soluble degradation products can be cleared by renal elimination [84].

2.5 Antiangiogenic agents loaded into DEE microspheres

Loading and elution of various antiangiogenic agents have been evaluated with DEE microspheres [30, 32, 85, 86] and performance of the loaded microspheres tested in preclinical models [27, 73, 79, 87, 88]. TACE-induced hypoxia can stimulate neoangiogenesis through increased expression of vascular endothelial growth factor (VEGF) which can lead to local tumor recurrence [89–91]. Antiangiogenic agents, such as the multikinase inhibitor sorafenib, have shown efficacy in HCC but are associated with systemic toxicities. Local delivery of these agents with DEE microspheres may be an effective strategy to mitigate systemic toxicity and inhibit neoangiogenic pathways induced by TACE.

2.6 Radiopaque DEE microspheres

Conventional DEE microspheres are radiolucent and thus cannot be directly visualized on intra-procedural fluoroscopy or other X-ray imaging modalities. Early imageable DEE microspheres were formulated by impregnating LC Bead with Lipiodol [92] enabling intra- and post-procedural visualization of the microspheres as demonstrated in preclinical models [93–95]. To address leaching of the entrapped Lipiodol from the microspheres over time, intrinsically radiopaque embolic microspheres were developed by conjugating a portion of the hydroxyl functional groups available on DC Bead with 2,3,5-triiodobenzoic acid via a linker [12]. Later, direct conjugation was achieved using 2,3,5-triiodobenzaldehyde [11, 13, 64]. These microspheres (DC Bead LUMI™) were shown to possess acceptable catheter deliverability, conspicuity on intra-procedural fluoroscopy, and persistent and stable image-ability on follow-up CT [11, 14, 64, 96]. It should be noted that the radiopaque microspheres do not shrink upon drug loading, in contrast to non-radiopaque DC Bead [97]. Recently, small diameter (40–90 μm) radiopaque microspheres were introduced to promote more distal arterial distribution [34].

Use of radiopaque DEE microspheres in humans has demonstrated real-time feedback regarding anatomic localization of microspheres during TACE [14, 98, 99]. Although the clinical utility of radiopaque DEE microspheres continues to be evaluated, it is postulated that they may facilitate refinement of treatment endpoint, visualization of non-target embolization, and early detection of undertreated regions of a tumor thus enabling same-procedure completion of treatment [14]. It has also been proposed that

microsphere radiopacity and distribution on imaging may serve as a surrogate for local drug concentrations enabling spatial drug dosimetry [15].

3. Drug effects and distribution following TACE with DEE microspheres

3.1 Drug vs ischemia

Results comparing the outcomes of embolization with bland microspheres and doxorubicin-loaded DEE microspheres have been mixed, fueling an ongoing debate as to the relative contributions of ischemia and drug to the efficacy of TACE [100]. There is evidence suggesting that both ischemia and drug may contribute to therapeutic effects. Some preclinical and clinical studies have demonstrated greater local cytotoxic effects surrounding DEE microspheres compared to bland microspheres [87, 101–104]. A retrospective study found that TACE with DEE microspheres loaded with epirubicin resulted in greater tumor necrosis compared to embolization with bland microspheres in embolized livers explanted for liver transplantation [105]. In a single center prospective randomized trial, TACE with DEE microspheres demonstrated superior time to progression than bland microspheres [69]. However, a single center randomized study by Brown *et al.* found no difference in response using RECIST 1.0 criteria as primary outcome between DEE microspheres and bland microsphere embolizations, although different bland and DEE microspheres were used [68].

3.2 Factors that influence drug distribution

To be most effective, chemotherapeutic agents must penetrate tissue effectively, maximizing the number of cells exposed to therapeutic drug concentrations. The extent to which this requirement applies to immunotherapeutic agents is not known, since exposure of discrete immunologic targets may be sufficient to stimulate systemic antitumor immune responses. There are a number of factors that contribute to the intratumoral distribution and effects of drugs delivered using DEE microspheres for TACE.

3.2.1 Microsphere distribution—Due to the relative colocalization of drug and microspheres, the extent of tumor drug coverage is largely dependent on the distribution of microspheres within the tumor vasculature. Indeed, the volume and attenuation of radiopaque DEE microspheres measured on CT in spatially discrete tumor samples was found to positively correlate with the amount of doxorubicin measured in the samples [15]. Upon injection, DEE microspheres are carried by blood flow and thus preferentially accumulate in regions of high arterial blood supply commonly associated with certain tumors. Smaller DEE microspheres become lodged more distally from the catheter within arteries and are therefore capable of providing superior drug coverage compared to larger microspheres prone to more proximal vessel occlusion [95, 106].

3.2.2 Drug release—To exert any effect, the drug must first be released from the microspheres. The amount of bioavailable drug, i.e. the fraction of drug eluted, in the tumor over time depends on the rate of drug release from the microspheres and rate of clearance from the tumor by washout or metabolism. *In vivo*, the drug release profile from DEE

microspheres may be defined by several phases with differing rate-determining mechanisms (Figure 1).

Drug release is most rapid immediately following DEE microsphere infusion, due in part to the high surface area of microspheres exposed to ions in blood and the “burst” release that is characteristic of initial drug release from DEE microspheres. As microspheres accumulate in arteries, blood flow is gradually reduced until flow stasis is reached and a microsphere-thrombus mass is formed. During this phase of the release profile, diffusion of ions into and drug out of the microspheres slows. Elevated drug levels in tissue immediately surrounding the microspheres may further reduce the rate of drug diffusion from the microspheres as the concentration gradient between the microspheres and surrounding tissue diminishes and equilibrates. This phenomenon may be particularly relevant for drugs that penetrate poorly into the tumor extravascular space, resulting in elevated concentrations in the immediate vicinity of the microspheres and prolonging drug release. In the case of doxorubicin, *in vivo* drug release can occur over a period of at least one month [108].

3.2.3 Tissue penetration—Intratumoral drug distribution is subject to a number of biologic barriers that can inhibit tumor drug penetration and coverage including large intervascular distances, dense cellular and extracellular compartments, and elevated interstitial fluid pressure (Figure 2). Drug transport in tumors is also influenced by the physicochemical characteristics of the drug including molecular size, charge, and solubility as well as the extent of cell uptake and binding [109–112]. Once released from DEE microspheres in tissues, drug transport is likely to occur predominantly by diffusion since convection is reduced or eliminated following embolization of blood vessels. Some studies have evaluated the distribution of drugs in tumors following embolization with DEE microspheres and found that doxorubicin remains within ~ 600 μm radially of the microspheres [15, 95, 103, 108], in contrast to sunitinib which penetrates further into surrounding tissues [113].

It is possible that tumor drug penetration following drug release from DEE microspheres may be improved by co-delivery of microenvironment modulators, such as drugs that normalize or remodel blood vessels or the extracellular matrix. Similarly, locoregional therapies (LRT) or other technologies, such as high intensity focused ultrasound or irreversible electroporation, may potentiate drug distribution by heating, convection, or mechanical disruption or permeabilization of tissue.

3.3 The tumor microenvironment

The tumor microenvironment plays an important role in determining local drug effects. Even if a drug is homogeneously distributed throughout a tumor, its effects may differ from one region to another due to spatial heterogeneity in cell phenotypes, proliferation rates, metabolism, and tissue oxygenation [114]. This may be particularly relevant for conventional cytostatic drugs that exert their effects in a cell cycle dependent manner. Tissue hypoxia induced by embolization may affect the susceptibility of cells to certain drugs such as doxorubicin, potentially increasing the dose required to achieve cytotoxic effects or selecting for a more aggressive tumor phenotype [115, 116]. However, the exact mechanisms

by which potential changes in the tumor microenvironment post-embolization, including possible alterations in interstitial fluid pressure, microvascular perfusion, and tumor stromal content, influence drug distribution and therapeutic effects require further exploration [117–120]. DEE microspheres loaded with hypoxia-activated or antiangiogenic drugs may be a promising strategy to exploit changes within the tumor microenvironment resulting from TACE.

3.4 Measuring drug distribution in tumors following TACE with DEE microspheres

A commonly employed method to assess drug accumulation in preclinical tumor models consists of tumor tissue homogenization, drug extraction, and quantification. Although this approach provides information regarding the total amount and concentration of drug in the entire tissue sample, information regarding the spatial distribution of drug in the sample is lost. For investigations of TACE with DEE microspheres, this approach additionally fails to differentiate between the eluted drug fraction, which is bioavailable, and the amount of drug sequestered in the microspheres, which does not contribute to the therapeutic effect. A number of techniques that rely on tissue homogenization have been employed to evaluate drug concentrations in tumors following TACE with DEE microspheres, but relatively few techniques have been used that preserve drug spatial distribution relative to the microspheres (Table 2).

For drugs that are naturally fluorescent, such as doxorubicin and sunitinib, spatial drug concentrations can be evaluated in tumor sections using fluorescence microscopy (Figure 3) [15, 95, 113]. However, quenching of fluorescence signal can restrict accurate quantification of the fraction of drug retained in the microspheres. To avoid this problem, infrared microspectroscopy has been used to quantify drugs inside microspheres and microspectrofluorimetry to detect drug in surrounding tissue [103].

For drugs that are not fluorescent, their distribution may be measured by radiolabeling, or, in some cases, inferred by assessing specific drug bioeffects as a surrogate [128]. For example, qPCR and microdissection were used to measure interleukin-6 in tissue as a marker of ibuprofen released by DEE microspheres [129].

4. DEE microspheres: emerging paradigms and innovations

4.1 Drug dosimetry

The advent of intrinsically radiopaque DEE microspheres has opened the door to the possibility of estimating spatial drug concentrations on intraprocedural CBCT or postprocedural CBCT or multidetector CT using microsphere radiopacity as a surrogate [130]. Recently, the volume and attenuation of radiopaque DEE microspheres measured on CT was shown to be linearly proportional to the amount of doxorubicin measured in liver samples in a rabbit model [15]. This correlation was then used to predict the amount of doxorubicin in the liver based on CT. One can imagine that similar models could enable real-time intraprocedural estimation of spatial drug dosimetry using CBCT to identify regions of tumor at risk of undertreatment (Figure 4). A limitation of this approach is that the ability to image radiopaque microsphere distribution clinically is limited by the

spatial resolution of imaging systems [131]. Further study is required to better understand the relationship between the imaged three-dimensional distribution of radiopaque DEE microspheres, drug distribution, and therapeutic effects of TACE. The ability to predict local drug levels could help to clarify the relative contributions of drug and ischemia to treatment efficacy.

4.2 Imaging of radiopaque DEE microspheres for rational drug targeting

The ability to image radiopaque microspheres with standard CBCT or multidetector CT is limited by the spatial resolution of both technologies [131]. The image is based on X-ray absorption alone and cannot be used to discriminate between different absorbers, such as calcium, iodine or bismuth. Spectral imaging with dual energy CT (DECT) generates two scans with different X-ray energy spectra that can be used to selectively identify a single k-edge absorber, e.g., iodine, in images and enables limited differentiation between two materials with different k-edge energies [132, 133]. Photon-counting CT systems under development use X-ray detectors that can quantify the number and energy of incident photons, enabling material decomposition for more than one radioabsorber, based on k-edges and measured absorption spectra [16, 134, 135]. These techniques could be used to differentiate DEE microspheres containing different radiopacifiers, such as iodine, bismuth or tantalum, from soluble contrast agents used during microsphere delivery or from each other. Furthermore, photon-counting CT systems offer higher spatial resolution than current CT scanners and may allow more complete imaging of radiopaque bead distribution [136].

Preliminary work on the synthesis of bismuth-containing microspheres and their differentiation on imaging from soluble iodinated contrast using DECT has been reported [17, 137]. Bismuth microspheres may be distinguished from iodine-based liquid contrast on photon counting CT and, by extension, from iodinated microspheres as its k-edge energy (90.52 KeV) is higher than that of iodine (33.2 KeV) [16, 135]. Although speculative, radiopaque DEE microspheres containing different radiopacifiers and loaded with different drugs could provide a means for rational targeting of different drugs to different regions of tumor based on their mechanisms of action, with the option to uniquely image their distribution with spectral or photon-counting CT (Figure 5).

4.3 DEE microspheres and immunomodulation

It has been hypothesized that the number of patients that respond to immunotherapy may be improved by combination with LRT such as transarterial chemoembolization, radioembolization, and thermal ablation (Figure 6) [138]. The rationale is that destruction of tumor cells induced by LRT may enhance tumor immunogenicity by promoting the expression of tumor-associated antigens and accumulation of tumor-infiltrating lymphocytes (TILs). Recently, augmentation of LRT-induced immune activation by concomitant systemic administration of check point inhibitors (CPI) was tested in a phase II trial and found to be safe and effective in a subset of patients with HCC refractory disease [139]. However, low response rates and systemic toxicities remain limiting characteristics of immunotherapy.

Strategies to increase tumor immunogenicity are being actively pursued in several clinical trials delivering CPI with antiangiogenic agents with or without LRT [140]. Among the

immune effects caused by antiangiogenic agents are restoration of dendritic cell maturation, and reduction of T-regulatory cells [141, 142]. Enhancement in recruitment and activation of CD8+ T cell response has also been reported [143–146]. A recent clinical study demonstrated better overall and progression-free survival for the systemic combination therapy of atezilumab, an anti-PD-L1 monoclonal antibody, and bevacizumab, an anti-VEGF monoclonal antibody, compared to sorafenib. However, severe adverse events were reported in 56% of the patients in the combination arm [147].

Another promising approach to augment antitumor immune responses is by pharmacologic targeting of immune stimulatory pathways including but not limited to STING, toll-like receptors (TLR) [148, 149], VISTA, TIM-3, Btk/Itk, and SHIP1 [150–152]. However, these agents have potentially serious non-target side effects when delivered systemically. Intratumoral bolus injection may require multiple or repeated administrations due to rapid clearance from the tumor and poor intratumoral distribution. DEE microspheres may enable better control of the pharmacokinetics and distribution of immune modulating agents, with the potential to approximate metronomic or continuous delivery schedules. To date, there is limited clinical experience with transarterial delivery of immune modulators [153–155].

There are currently a number of clinical trials underway exploring the combination of LRT with immunotherapy [156]. The potential systemic toxicity of many immune-modulating agents suggests that they may be ideal candidates for tumor-localized delivery with DEE microspheres. However, loading of monoclonal antibodies in DEE microspheres is poor. Recently, small molecule CPI targeting the PD-1/PD-L1 pathway have been developed that may provide greater flexibility of route of administration, improved toxicity profiles, and reduced costs compared to antibody-based CPIs [157, 158]. However, more research is needed to effectively combine immune modulating agents with DEE microspheres and to optimize drug selection, loading, and elution profiles.

5. Expert opinion

TACE is a minimally-invasive LRT that employs catheters and imaging-based vascular “roadmaps” to deliver therapy directly to tumors, precisely where it is needed. This exquisite access to tumors presents vast opportunities for locoregional drug delivery using controlled release drug delivery systems, such as DEE microspheres, to reduce systemic drug exposure, increase intratumoral drug concentrations, and provide greater control over spatial and temporal drug distribution.

Doxorubicin remains the most commonly used drug for TACE despite its abandonment as a systemic treatment for HCC and evidence suggesting other drugs may have greater activity *in vitro* [159]. Outcomes of trials comparing drug-loaded microspheres to bland microspheres have been mixed, further fueling the debate as to the contribution of doxorubicin to treatment efficacy and whether it is the optimal drug for delivery with DEE microspheres. Nevertheless, pre-treatment biopsies may soon dictate rational drug selection, based on single cell transcriptomics with clusters of common mutations or RNA expression patterns that define susceptibilities to TACE [160]. Yet, mutational heterogeneity within a

single tumor and between synchronous multifocal tumors may limit the ability to capture the full mutational landscape with a single biopsy specimen.

A similar scenario may be envisioned in which drug selection could be informed non-invasively using imaging features to identify potential therapeutic targets. For instance, multi-parametric AI and deep learning models trained with digital pathology, genomic data, and imaging could potentially identify the most effective combination of DEE microspheres and drugs, and where to deliver them, based on pre-treatment imaging. Indeed, different drugs could be specifically delivered to discrete regions of tumors based on surrogate imaging markers that correlate with specific tumor phenotypes, molecular signatures, or immunologic status. Imageable DEE microspheres containing different radiopacifiers distinguishable using photon counting CT could facilitate image-guided spatial drug delivery of multiple agents.

As our understanding of post-embolization changes in the tumor microenvironment grows, so do the opportunities to use drugs that specifically target local conditions created by TACE. Tumor hypoxia may be a double edge sword: a natural consequence of ischemia induced by embolization that causes necrosis, but also a promoter of neoangiogenesis leading to local recurrence. The hypoxic microenvironment may present a rationale for use of hypoxia-activated drugs or other targeted agents as a means to enhance drug efficacy. Vascular agents that target VEGF or hypoxia-inducible factor 1-alpha (HIF1alpha) may serve to limit angiogenesis induced by tumor hypoxia, regarded as a mechanism of local tumor recurrence after TACE, or even promote beneficial antitumor immune effects. A number of multikinase inhibitors of various other pathways remain to be explored in combination with DEE microspheres and present numerous intriguing possibilities for local delivery. Counteracting mediators of pro-oncogenic effects following LRT such as TACE, for example by suppressing tumor stress responses by local delivery of inhibitors using DEE microspheres, may also be possible [161].

The recent success of immunotherapy in the form of checkpoint inhibitors has ushered in a new era of cancer therapy. However, many of these treatments are limited by poor response rates and undesirable systemic and non-target effects. There is growing evidence that response rates to immunotherapy may be augmented by LRT, based on the observation that LRT may elicit immunologic cell death and enhance tumor-antigen presentation. In this way, LRT and local administration of immune modulating agents, for example by delivery using DEE microspheres (“immunobeads”), may help to convert tumors from immunologically “cold” desert or immune-excluded tumors to “hot” and immune-susceptible, in order to expand the number of patients that may benefit from immunotherapy. Heterogeneous regions of tumors with more aggressive and active clonality or neoantigens could be identified with imaging, then targeted for destruction or enhancement of antigen release and presentation via TACE, ablation, or DEE microspheres loaded with immune modulators.

The diverse types of immune cells, receptors, and molecular pathways that could potentially be targeted by drugs presents a wealth of opportunities for local drug delivery with DEE microspheres. Many of these agents may be used to target specific inherent tumor characteristics, potentially identified by next-generation sequencing technologies, or

biologic processes initiated by TACE itself. As we move beyond the use of conventional chemotherapeutic agents for TACE, an emphasis on systematic comparative preclinical and clinical studies, supported by collaborative, inter-disciplinary research efforts, will be crucial to expedite the translation of next-generation DEE microsphere–drug combinations for clinical use.

Funding

This work was supported by the NIH Center for Interventional Oncology and the Intramural Research Program of the National Institutes of Health via intramural NIH Grants Z1A CL040015, 1ZIDBC011242. Dr. Mauda-Havakuk is supported by the Intramural Research Program of the National Institute of Biomedical Imaging and Bioengineering.

Abbreviations

cTACE	Conventional Transarterial Chemoembolization
CPI	checkpoint inhibitor
DEB	Drug-eluting bead
DECT	dual energy CT
DEE	drug-eluting embolic
HCC	hepatocellular carcinoma
LRT	locoregional therapy
PCCT	photon counting CT
TACE	transarterial chemoembolization
TLR	toll-like receptor
VEGF	vascular endothelial growth factor

References

Papers of special note have been highlighted as:

* of interest

** of considerable interest

1. Dasgupta P, Henshaw C, Youlden DR, et al. Global Trends in Incidence Rates of Primary Adult Liver Cancers: A Systematic Review and Meta-Analysis. *Front Oncol* 2020;10.
2. Galle PR, Forner A, Llovet JM, et al. EASL Clinical Practice Guidelines: Management of hepatocellular carcinoma. *J Hepatol* 2018;69:182–236. [PubMed: 29628281]
3. Fiorentini G, Aliberti C, Tilli M, et al. Intra-arterial infusion of irinotecan-loaded drug-eluting beads (DEBIRI) versus intravenous therapy (FOLFIRI) for hepatic metastases from colorectal cancer: final results of a phase III study. *Anticancer Res* 2012;32:1387–95. [PubMed: 22493375]
4. Martin RC, Robbins K, Fagés JF, et al. Optimal outcomes for liver-dominant metastatic breast cancer with transarterial chemoembolization with drug-eluting beads loaded with doxorubicin. *Breast Cancer Res Treat* 2012;132:753–63. [PubMed: 22200868]

5. Rostas J, Tam A, Sato T, et al. Image-guided transarterial chemoembolization with drug-eluting beads loaded with doxorubicin (DEBDOX) for unresectable hepatic metastases from melanoma: technique and outcomes. *Cardiovasc Intervent Radiol* 2017;40:1392–400. [PubMed: 28508253]
6. D'Souza D, Golzarian J, Young S. Interventional Liver-Directed Therapy for Neuroendocrine Metastases: Current Status and Future Directions. *Current Treatment Options in Oncology* 2020;21:52. [PubMed: 32447461]
7. Gupta S, Wright KC, Ensor J, et al. Hepatic arterial embolization with doxorubicin-loaded superabsorbent polymer microspheres in a rabbit liver tumor model. *Cardiovasc Intervent Radiol* 2011;34:1021–30. [PubMed: 21479746]
8. Taylor RR, Tang Y, Gonzalez MV, et al. Irinotecan drug eluting beads for use in chemoembolization: in vitro and in vivo evaluation of drug release properties. *Eur J Pharm Sci* 2007;30:7–14. [PubMed: 17030118]
9. Varela M, Real MI, Burrell M, et al. Chemoembolization of hepatocellular carcinoma with drug eluting beads: efficacy and doxorubicin pharmacokinetics. *J Hepatol* 2007;46:474–81. [PubMed: 17239480] ** Important study in patients with HCC demonstrating reduced Cmax and AUC for TACE with DEE microspheres loaded with doxorubicin compared to conventional TACE.
10. Poon RT, Tso WK, Pang RW, et al. A phase I/II trial of chemoembolization for hepatocellular carcinoma using a novel intra-arterial drug-eluting bead. *Clin Gastroenterol Hepatol* 2007;5:1100–8. [PubMed: 17627902] ** Important phase I/II clinical trial demonstrating reduced systemic exposure of TACE with DEE microsphere loaded with doxorubicin compared to historical data for intraarterial delivery of free drug or drug emulsified with Lipiodol.
11. Duran R, Sharma K, Dreher MR, et al. A novel inherently radiopaque bead for transarterial embolization to treat liver cancer - A pre-clinical study. *Theranostics* 2016;6:28–39. [PubMed: 26722371] * Characterization of physicochemical properties, deliverability, and visibility on imaging of intrinsically radiopaque DEE microspheres in the rabbit VX2 model.
12. Negussie AH, Dreher MR, Johnson CG, et al. Synthesis and characterization of image-able polyvinyl alcohol microspheres for image-guided chemoembolization. *J Mater Sci Mater Med* 2015;26:198. [PubMed: 26105830] * Study demonstrating synthesis of intrinsically radiopaque DEE microspheres.
13. Ashrafi K, Tang Y, Britton H, et al. Characterization of a novel intrinsically radiopaque drug-eluting bead for image-guided therapy: DC Bead LUMI. *J Control Release* 2017;250:36–47. [PubMed: 28188808] * Report demonstrating preparation and characterization of intrinsically radiopaque DEE microspheres.
14. Levy EB, Krishnasamy VP, Lewis AL, et al. First human experience with directly image-able iodinated embolization microbeads. *Cardiovasc Intervent Radiol* 2016;39:1177–86. [PubMed: 27206503] ** Report of first in human use of radiopaque DEE microspheres
15. Mikhail AS, Pritchard WF, Negussie AH, et al. Mapping drug dose distribution on CT images following transarterial chemoembolization with radiopaque drug-eluting beads in a rabbit tumor model. *Radiology* 2018;289:396–404. [PubMed: 30106347] ** First report demonstrating the potential feasibility of drug dose mapping following chemoembolization with radiopaque DEE microspheres. The radiopacity of the microspheres on CT imaging was used to estimate drug concentrations in rabbit VX2 liver tumors.
16. Spectral photon-counting CT: Spatial differentiation of static contrast versus radiopaque image-able drug eluting microspheres. Pourmorteza A, Negussie AH, Symons R, et al. *Radiological Society of North America 2016 Scientific Assembly and Annual Meeting 2016*; Available at: archive.rsna.org/2016/16014790.html [cited September 8 2020]
17. Negussie AH, De Ruyter Q, Britton H, et al. Bismuth based Image-able Microspheres: First Application for use in Dual Energy Computed Tomography for Image-Guided Therapeutic Embolization. *European Molecular Imaging Meeting*. Glasgow, UK 2019.
18. Lindell B, Aronsen K-F, Nosslin B, et al. Studies in pharmacokinetics and tolerance of substances temporarily retained in the liver by microsphere embolization. *Ann Surg* 1978;187:95–99. [PubMed: 619805]
19. Aronsen KF, Hellekant C, Holmberg J, et al. Controlled blocking of hepatic artery flow with enzymatically degradable microspheres combined with oncolytic drugs. *Eur Surg Res* 1979;11:99–106. [PubMed: 385325]

20. Lammer J, Malagari K, Vogl T, et al. Prospective randomized study of doxorubicin-eluting-bead embolization in the treatment of hepatocellular carcinoma: results of the PRECISION V study. *Cardiovasc Intervent Radiol* 2010;33:41–52. [PubMed: 19908093]
21. Wang C-y, Xia J-g, Yang Z-q, et al. Transarterial chemoembolization with medium-sized doxorubicin-eluting Callisphere is safe and effective for patients with hepatocellular carcinoma. *Sci Rep* 2020;10:4434. [PubMed: 32157110]
22. Liang B, Xiang H, Ma C, et al. Comparison of chemoembolization with callispheres[®] microspheres and conventional chemoembolization in the treatment of hepatocellular carcinoma: A multicenter retrospective study. *Cancer Manag Res* 2020;12:941–56. [PubMed: 32104076]
23. Zhou G-H, Han J, Sun J-H, et al. Efficacy and safety profile of drug-eluting beads transarterial chemoembolization by CalliSpheres[®] beads in Chinese hepatocellular carcinoma patients. *BMC Cancer* 2018;18:644. [PubMed: 29914435]
24. Lewis AL, Taylor RR, Hall B, et al. Pharmacokinetic and safety study of doxorubicin-eluting beads in a porcine model of hepatic arterial embolization. *J Vasc Interv Radiol* 2006;17:1335–43. [PubMed: 16923981] ** Important early study demonstrating pathologic and pharmacokinetic findings from hepatic embolization with doxorubicin-eluting beads in a porcine model.
25. Spindeldreier KC, Thiesen J, Kraemer I. Loading, release and stability of epirubicin-loaded drug-eluting beads. *J Oncol Pharm Pract* 2016;22:591–98. [PubMed: 26160072]
26. Lahti SJ, Zeng D, Jia JB, et al. Sorafenib loaded drug-eluting beads: loading and eluting kinetics and in vitro viability study. *J Vasc Interv Radiol* 2015;26:S80–S81.
27. Fuchs K, Bize PE, Dormond O, et al. Drug-eluting beads loaded with antiangiogenic agents for chemoembolization: in vitro sunitinib loading and release and in vivo pharmacokinetics in an animal model. *J Vasc Interv Radiol* 2014;25:379–87.e1–2. [PubMed: 24468044]
28. Boulin M, Hillon P, Cercueil JP, et al. Idarubicin-loaded beads for chemoembolisation of hepatocellular carcinoma: results of the IDASPHERE phase I trial. *Aliment Pharmacol Ther* 2014;39:1301–13. [PubMed: 24738629]
29. Forster RE, Small SA, Tang Y, et al. Comparison of DC Bead-irinotecan and DC Bead-topotecan drug eluting beads for use in locoregional drug delivery to treat pancreatic cancer. *J Mater Sci Mater Med* 2010;21:2683–90. [PubMed: 20563626]
30. Sakr OS, Berndt S, Carpentier G, et al. Arming embolic beads with anti-VEGF antibodies and controlling their release using LbL technology. *J Control Release* 2016;224:199–207. [PubMed: 26780173]
31. Keese M, Gasimova L, Schwenke K, et al. Doxorubicin and mitoxantrone drug eluting beads for the treatment of experimental peritoneal carcinomatosis in colorectal cancer. *Int J Cancer* 2009;124:2701–08. [PubMed: 19165866]
32. Hagan A, Phillips GJ, Macfarlane WM, et al. Preparation and characterisation of vandetanib-eluting radiopaque beads for locoregional treatment of hepatic malignancies. *Eur J Pharm Sci* 2017;101:22–30. [PubMed: 28132823]
33. Krishnasamy V, Banovac F, Mikhail A, et al. Topotecan-eluting radiopaque embolic beads (ROB) for transarterial hepatic chemoembolization (TACE). *J Vasc Interv Radiol* 2016;27:S130.
34. Lewis AL, Caine M, Garcia P, et al. Handling and performance characteristics of a new small caliber radiopaque embolic microsphere. *J Biomed Mater Res B Appl Biomater* 2020;Online ahead of print.
35. Gnutzmann DM, Mechel J, Schmitz A, et al. Evaluation of the plasmatic and parenchymal elution kinetics of two different irinotecan-loaded drug-eluting embolics in a pig model. *J Vasc Interv Radiol* 2015;26:746–54. [PubMed: 25704223]
36. Richter G, Radeleff B, Stroszczyński C, et al. Safety and feasibility of chemoembolization with doxorubicin-loaded small calibrated microspheres in patients with hepatocellular carcinoma: Results of the MIRACLE I prospective multicenter study. *Cardiovasc Intervent Radiol* 2018;41:587–93. [PubMed: 29167967]
37. Guiu B, Hincapie G, Thompson L, et al. An in vitro evaluation of four types of drug-eluting embolics loaded with idarubicin. *J Vasc Interv Radiol* 2019;30:1303–09. [PubMed: 31155500]

38. Sottani C, Poggi G, Quaretti P, et al. Serum pharmacokinetics in patients treated with transarterial chemoembolization (TACE) using two types of epirubicin-loaded microspheres. *Anticancer Res* 2012;32:1769–74. [PubMed: 22593459]
39. Poggi G, Quaretti P, Minoia C, et al. Transhepatic arterial chemoembolization with oxaliplatin-eluting microspheres (OEM-TACE) for unresectable hepatic tumors. *Anticancer Res* 2008;28:3835–42. [PubMed: 19192637]
40. Chen M, Xu R, Chen X, et al. Hepatic fibrosis and short-term clinical efficacy after hepatic artery embolization for unresectable hepatocellular carcinoma using doxorubicin-eluting HepaSphere. *Transl Cancer Res* 2020;9:1361–70. [PubMed: 35117484]
41. Seki A, Hori S. Switching the loaded agent from epirubicin to cisplatin: Salvage transcatheter arterial chemoembolization with drug-eluting microspheres for unresectable hepatocellular carcinoma. *Cardiovasc Intervent Radiol* 2012;35:555–62. [PubMed: 21562932]
42. Namur J, Pascale F, Maeda N, et al. Safety and efficacy compared between irinotecan-loaded microspheres HepaSphere and DC bead in a model of VX2 liver metastases in the rabbit. *J Vasc Interv Radiol* 2015;26:1067–75.e3. [PubMed: 25952641]
43. Jiaqi Y, S H, K M, et al. [A new embolic material: super absorbent polymer (SAP) microsphere and its embolic effects]. *Nihon Igaku Hoshasen Gakkai Zasshi* 1996;56:19–24. [PubMed: 8857094]
44. de Baere T, Plotkin S, Yu R, et al. An in vitro evaluation of four types of drug-eluting microspheres loaded with doxorubicin. *J Vasc Interv Radiol* 2016;27:1425–31. [PubMed: 27402527] * Study demonstrating head-to-head comparison of doxorubicin *in vitro* release kinetics using commercially available DEE microspheres.
45. Pereira PL, Plotkin S, Yu R, et al. An in-vitro evaluation of three types of drug-eluting microspheres loaded with irinotecan. *Anticancer drugs* 2016;27:873–8. [PubMed: 27416270]
46. Gjoreski A, Popova-Jovanovska R, Eftimovska-Rogac I, et al. Safety profile and efficacy of chemoembolization with doxorubicin-loaded polyethylene glycol microspheres in patients with hepatocellular carcinoma. *Open Access Maced J Med Sci* 2019;7:742–46. [PubMed: 30962831]
47. Terumo's BioPearl, the First Biodegradable Drug Eluting Microspheres Received CE mark. 2020; Available at: <https://www.terumo.com/pressrelease/detail/20200428/530/index.html> [cited June 17 2020]
48. Lewis AL. DC Bead: a major development in the toolbox for the interventional oncologist. *Expert Rev Med Devices* 2009;6:389–400. [PubMed: 19572794]
49. Lewis AL, Gonzalez ÆMV, Leppard SW, et al. Doxorubicin eluting beads – 1 : Effects of drug loading on bead characteristics and drug distribution. *J Mater Sci Mater Med* 2007;18:1691–99. [PubMed: 17483878]
50. Abdekhodaie MJ, Wu XY. Drug loading onto ion-exchange microspheres: Modeling study and experimental verification. *Biomaterials* 2006;27:3652–62. [PubMed: 16516960]
51. Jordan O, Denys A, De Baere T, et al. Comparative study of chemoembolization loadable beads: In vitro drug release and physical properties of DC Bead and Hepasphere loaded with doxorubicin and irinotecan. *J Vasc Interv Radiol* 2010;21:1084–90. [PubMed: 20610183]
52. Gonzalez MV, Tang Y, Phillips GJ, et al. Doxorubicin eluting beads-2: methods for evaluating drug elution and in-vitro:in-vivo correlation. *J Mater Sci Mater Med* 2008;19:767–75. [PubMed: 17653626] * Report demonstrating the role of an ion-exchange mechanism in controlling doxorubicin release from DEE microspheres.
53. Ahnfelt E, Sjögren E, Hansson P, et al. In vitro release mechanisms of doxorubicin from a clinical bead drug-delivery system. *J Pharm Sci* 2016;105:3387–98. [PubMed: 27663384] * Thorough study evaluating mechanisms of drug release from DEE microspheres, and the effects of various parameters and conditions *in vitro*.
54. Biondi M, Fusco S, Lewis AL, et al. Investigation of the mechanisms governing doxorubicin and irinotecan release from drug-eluting beads: mathematical modeling and experimental verification. *J Mater Sci Mater Med* 2013;24:2359–70. [PubMed: 23797828]
55. Lewis AL, Dreher MR, O'Byrne V, et al. DC BeadTM : towards an optimal transcatheter hepatic tumour therapy. *J Mater Sci Mater Med* 2016;27:1–12. [PubMed: 26610924]
56. Ahnfelt E, Gernandt J, Al-Tikriti Y, et al. Single bead investigation of a clinical drug delivery system – A novel release mechanism. *J Control Release* 2018;292:235–47. [PubMed: 30419268]

57. United States Pharmacopeia. <711> Dissolution. Rockville, MD: United States Pharmacopeial Convention 2016.
58. Hu J, Albadawi H, Chong BW, et al. Advances in biomaterials and technologies for vascular embolization. *Adv Mater* 2019;31:1901071.
59. Wassef M, Pelage J-P, Velzenberger E, et al. Anti-inflammatory effect of ibuprofen-loaded embolization beads in sheep uterus. *Journal of Biomedical Materials Research Part B: Applied Biomaterials* 2008;86:63–73. [PubMed: 18098185]
60. Forster RE, Tang Y, Bowyer C, et al. Development of a combination drug-eluting bead: towards enhanced efficacy for locoregional tumour therapies. *Anticancer drugs* 2012;23:355–69. [PubMed: 22241169]
61. Jones RP, Malik HZ, Fenwick SW, et al. PARAGON II - A single arm multicentre phase II study of neoadjuvant therapy using irinotecan bead in patients with resectable liver metastases from colorectal cancer. *Eur J Surg Oncol* 2016;42:1866–72. [PubMed: 27561844]
62. Levy EB, Peer C, Sissung TM, et al. Pilot study comparing systemic and tissue pharmacokinetics of irinotecan and metabolites after hepatic drug-eluting chemoembolization. *J Vasc Interv Radiol* 2019;30:19–22. [PubMed: 30527657]
63. Beaton L, Tregidgo HFJ, Znati SA, et al. VEROnA protocol: A pilot, open-label, single-arm, phase 0, window-of-opportunity study of vandetanib-eluting radiopaque embolic beads (BTG-002814) in patients with resectable liver malignancies. *JMIR Res Protoc* 2019;8:e13696. [PubMed: 31579027]
64. Sharma KV, Bascal Z, Kilpatrick H, et al. Long-term biocompatibility, imaging appearance and tissue effects associated with delivery of a novel radiopaque embolization bead for image-guided therapy. *Biomaterials* 2016;103:293–304. [PubMed: 27419364]
65. Denys A, Czuczman P, Grey D, et al. Vandetanib-eluting radiopaque beads: In vivo pharmacokinetics, safety and toxicity evaluation following swine liver embolization. *Theranostics* 2017;7:2164–76. [PubMed: 28740542]
66. Stampfl U, Stampfl S, Bellemann N, et al. Experimental liver embolization with four different spherical embolic materials: Impact on inflammatory tissue and foreign body reaction. *Cardiovasc Intervent Radiol* 2009;32:303–12. [PubMed: 19139955]
67. Golfieri R, Giampalma E, Renzulli M, et al. Randomised controlled trial of doxorubicin-eluting beads vs conventional chemoembolisation for hepatocellular carcinoma. *Br J Cancer* 2014;111:255–64. [PubMed: 24937669]
68. Brown KT, Do RK, Gonen M, et al. Randomized trial of hepatic artery embolization for hepatocellular carcinoma using doxorubicin-eluting microspheres compared with embolization with microspheres alone. *J Clin Oncol* 2016;34:2046–53. [PubMed: 26834067] ** An important prospective, single-center, randomized trial comparing the outcome of embolization using bland microspheres with chemoembolization using doxorubicin-eluting microspheres
69. Malagari K, Pomoni M, Kelekis A, et al. Prospective randomized comparison of chemoembolization with doxorubicin-eluting beads and bland embolization with BeadBlock for hepatocellular carcinoma. *Cardiovasc Intervent Radiol* 2010;33:541–51. [PubMed: 19937027] ** An important prospective, randomized trial comparing embolization using bland microspheres to chemoembolization using doxorubicin-eluting microspheres
70. Vogl TJ, Lammer J, Lencioni R, et al. Liver, gastrointestinal, and cardiac toxicity in intermediate hepatocellular carcinoma treated with PRECISION TACE with drug-eluting beads: Results from the PRECISION V randomized trial. *AJR Am J Roentgenol* 2011;197:W562–W70. [PubMed: 21940527]
71. Mikhail AS, Levy EB, Krishnasamy VP, et al. Safety and tolerability of topotecan-eluting radiopaque microspheres for hepatic chemoembolization in a rabbit preclinical model. *Cardiovasc Intervent Radiol*. Epub ahead of print 16 Aug 2020.
72. Gholamrezanezhad A, Mirpour S, Geschwind JF, et al. Evaluation of 70–150µm doxorubicin-eluting beads for transcatheter arterial chemoembolization in the rabbit liver VX2 tumour model. *Eur Radiol* 2016;26:3474–82. [PubMed: 26780638]
73. Bize P, Duran R, Fuchs K, et al. Antitumoral effect of sunitinib-eluting beads in the rabbit VX2 tumor model. *Radiology* 2016;280:425–35. [PubMed: 26919561]

74. Weng L, Rostamzadeh P, Nooryshokry N, et al. In vitro and in vivo evaluation of biodegradable embolic microspheres with tunable anticancer drug release. *Acta Biomater* 2013;9:6823–33. [PubMed: 23419554]
75. van Elk M, Ozbakir B, Barten-Rijbroek AD, et al. Alginate microspheres containing temperature sensitive liposomes (TSL) for MR-guided embolization and triggered release of doxorubicin. *PLoS One* 2015;10:e0141626. [PubMed: 26561370]
76. Yan J, Wang F, Chen J, et al. Preparation and characterization of irinotecan loaded cross-linked bovine serum albumin beads for liver cancer chemoembolization therapy. *Int J Polym Sci* 2016;9651486.
77. Weng L, Tseng HJ, Rostamzadeh P, et al. In vitro comparative study of drug loading and delivery properties of bioresorbable microspheres and LC bead. *J Mater Sci Mater Med* 2016;27:174. [PubMed: 27752972]
78. Wang Y, Molin DGM, Sevrin C, et al. In vitro and in vivo evaluation of drug-eluting microspheres designed for transarterial chemoembolization therapy. *Int J Pharm* 2016;503:150–62. [PubMed: 26965198]
79. Chen J, White SB, Harris KR, et al. Poly(lactide-co-glycolide) microspheres for MRI-monitored delivery of sorafenib in a rabbit VX2 model. *Biomaterials* 2015;61:299–306. [PubMed: 26022791]
80. Choi JW, Park JH, Cho HR, et al. Sorafenib and 2,3,5-triiodobenzoic acid-loaded imageable microspheres for transarterial embolization of a liver tumor. *Sci Rep* 2017;7:554. [PubMed: 28373713]
81. Okamoto Y, Hasebe T, Bito K, et al. Fabrication of radiopaque drug-eluting beads based on Lipiodol/biodegradable-polymer for image-guided transarterial chemoembolization of unresectable hepatocellular carcinoma. *Polym Degrad* 2020;175:109106.
82. Louguet S, Verret V, Bédouet L, et al. Poly(ethylene glycol) methacrylate hydrolyzable microspheres for transient vascular embolization. *Acta Biomater* 2014;10:1194–205. [PubMed: 24321348]
83. Verret V, Pelage JP, Wassef M, et al. A novel resorbable embolization microsphere for transient uterine artery occlusion: a comparative study with trisacryl-gelatin microspheres in the sheep model. *J Vasc Interv Radiol* 2014;25:1759–66. [PubMed: 25194456]
84. Yamaoka T, Tabata Y, Ikada Y. Fate of water-soluble polymers administered via different routes. *J Pharm Sci* 1995;84:349–54. [PubMed: 7616376]
85. Lahti S, Ludwig JM, Xing M, et al. In vitro biologic efficacy of sunitinib drug-eluting beads on human colorectal and hepatocellular carcinoma-A pilot study. *PLoS One* 2017;12:e0174539. [PubMed: 28384190]
86. Bédouet L, Verret V, Louguet S, et al. Anti-angiogenic drug delivery from hydrophilic resorbable embolization microspheres: an in vitro study with sunitinib and bevacizumab. *Int J Pharm* 2015;484:218–27. [PubMed: 25701631]
87. Duran R, Namur J, Pascale F, et al. Vandetanib-eluting radiopaque beads: Pharmacokinetics, safety, and efficacy in a rabbit model of liver cancer. *Radiology* 2019;293:695–703. [PubMed: 31617791]
88. Li X, He G, Su F, et al. Regorafenib-loaded poly (lactide-co-glycolide) microspheres designed to improve transarterial chemoembolization therapy for hepatocellular carcinoma. *Asian J Pharm Sci*. Epub ahead of print 19 Feb 2020.
89. Shim JH, Park J-W, Kim JH, et al. Association between increment of serum VEGF level and prognosis after transcatheter arterial chemoembolization in hepatocellular carcinoma patients. *Cancer Sci* 2008;99:2037–44. [PubMed: 19016764]
90. Li X, Feng G-S, Zheng C-S, et al. Expression of plasma vascular endothelial growth factor in patients with hepatocellular carcinoma and effect of transcatheter arterial chemoembolization therapy on plasma vascular endothelial growth factor level. *World J Gastroenterol* 2004;10:2878–82. [PubMed: 15334691]
91. Sergio A, Cristofori C, Cardin R, et al. Transcatheter arterial chemoembolization (TACE) in hepatocellular carcinoma (HCC): the role of angiogenesis and invasiveness. *Am J Gastroenterol* 2008;103:914–21. [PubMed: 18177453]
92. Johnson CG, Tang Y, Beck A, et al. Preparation of radiopaque drug-eluting beads for transcatheter chemoembolization. *J Vasc Interv Radiol* 2016;27:117–26.e3. [PubMed: 26549370]

93. Sharma KV, Dreher MR, Tang Y, et al. Development of “imageable” beads for transcatheter embolotherapy. *J Vasc Interv Radiol* 2010;21:865–76. [PubMed: 20494290]
94. Tacher V, Duran R, Lin M, et al. Multimodality imaging of ethiodized oil–loaded radiopaque microspheres during transarterial embolization of rabbits with VX2 liver tumors. *Radiology* 2016;279:741–53. [PubMed: 26678453]
95. Dreher MR, Sharma KV, Woods DL, et al. Radiopaque drug-eluting beads for transcatheter embolotherapy: experimental study of drug penetration and coverage in swine. *J Vasc Interv Radiol* 2012;23:257–64.e4. [PubMed: 22178039] ** Important study demonstrating the kinetics of doxorubicin distribution relative to DEE microspheres in swine liver.
96. Lewis AL, Willis SL, Dreher MR, et al. Bench-to-clinic development of imageable drug-eluting embolization beads: finding the balance. *Future Oncol* 2018;14:2741–60. [PubMed: 29944007]
97. Lewis AL, Gonzalez MV, Lloyd AW, et al. DC bead: in vitro characterization of a drug-delivery device for transarterial chemoembolization. *J Vasc Interv Radiol* 2006;17:335–42. [PubMed: 16517780]
98. Aliberti C, Carandina R, Sarti D, et al. Transarterial chemoembolization with DC Bead LUMI™ radiopaque beads for primary liver cancer treatment: preliminary experience. *Future Oncol* 2017;13:2243–52. [PubMed: 29063780]
99. Reicher J, Mafeld S, Priona G, et al. Early experience of trans-arterial chemo-embolisation for hepatocellular carcinoma with a novel radiopaque bead. *Cardiovasc Intervent Radiol* 2019;42:1563–70. [PubMed: 31455987]
100. Boulin M, Guiu B. Chemoembolization or bland embolization for hepatocellular carcinoma: the question is still unanswered. *J Clin Oncol* 2017;35:256–57.
101. Gaba RC, Emmadi R, Parvinian A, et al. Correlation of doxorubicin delivery and tumor necrosis after drug-eluting bead transarterial chemoembolization of rabbit VX2 liver tumors. *Radiology* 2016;280:752–61. [PubMed: 26967144]
102. Lee KH, Liapi EA, Cornell C, et al. Doxorubicin-loaded QuadraSphere microspheres: plasma pharmacokinetics and intratumoral drug concentration in an animal model of liver cancer. *Cardiovasc Intervent Radiol* 2010;33:576–82. [PubMed: 20087738]
103. Namur J, Wassef M, Millot J-M, et al. Drug-eluting beads for liver embolization: concentration of doxorubicin in tissue and in beads in a pig model. *J Vasc Interv Radiol* 2010;21:259–67. [PubMed: 20123210] ** Important study demonstrating the *in vivo* release and distribution of doxorubicin relative to DEE microspheres in swine liver. Quantification of doxorubicin concentration inside the microspheres using infrared microspectroscopy is also demonstrated.
104. Klass D, Owen D, Buczkowski A, et al. The effect of doxorubicin loading on response and toxicity with drug-eluting embolization in resectable hepatoma: A dose escalation study. *Anticancer Res* 2014;34:3597–606. [PubMed: 24982375]
105. Nicolini A, Martinetti L, Crespi S, et al. Transarterial chemoembolization with epirubicin-eluting beads versus transarterial embolization before liver transplantation for hepatocellular carcinoma. *J Vasc Interv Radiol* 2010;21:327–32. [PubMed: 20097098]
106. Caine M, Zhang X, Hill M, et al. Comparison of microsphere penetration with LC Bead LUMI versus other commercial microspheres. *J Mech Behav Biomed Mater* 2018;78:46–55. [PubMed: 29132100]
107. Hagan A, Caine M, Press C, et al. Predicting pharmacokinetic behaviour of drug release from drug-eluting embolization beads using in vitro elution methods. *Eur J Pharm Sci* 2019;136:104943. [PubMed: 31152772]
108. Namur J, Citron SJ, Sellers MT, et al. Embolization of hepatocellular carcinoma with drug-eluting beads: doxorubicin tissue concentration and distribution in patient liver explants. *J Hepatol* 2011;55:1332–8. [PubMed: 21703190] ** Rare report of doxorubicin distribution and tissue pharmacokinetics in transplanted human livers after embolization of HCC tumors with DEE microspheres.
109. Chauhan VP, Stylianopoulos T, Boucher Y, et al. Delivery of molecular and nanoscale medicine to tumors: transport barriers and strategies. *Annu Rev Chem Biomol Eng* 2011;2:281–98. [PubMed: 22432620]

110. Dewhirst MW, Secomb TW. Transport of drugs from blood vessels to tumour tissue. *Nat Rev Cancer* 2017;17:738–50. [PubMed: 29123246]
111. Minchinton AI, Tannock IF. Drug penetration in solid tumours. *Nat Rev Cancer* 2006;6:583–92. [PubMed: 16862189] ** Excellent review of factors that influence drug distribution in solid tumors, models to assess drug penetration, and potential strategies to overcome barriers to drug transport.
112. Netti PA, Berk DA, Swartz MA, et al. Role of extracellular matrix assembly in interstitial transport in solid tumors. *Cancer Res* 2000;60:2497–503. [PubMed: 10811131]
113. Fuchs K, Kiss A, Bize PE, et al. Mapping of drug distribution in the rabbit liver tumor model by complementary fluorescence and mass spectrometry imaging. *J Control Release* 2018;269:128–35. [PubMed: 29101054] * Study evaluating the distribution of sunitinib in rabbit VX2 tumors relative to beads using several methods including fluorescence microscopy mass spectroscopy imaging and LC-MS/MS.
114. Trédan O, Galmarini CM, Patel K, et al. Drug resistance and the solid tumor microenvironment. *J Natl Cancer Inst* 2007;99:1441–54. [PubMed: 17895480]
115. Dubbelboer IR, Pavlovic N, Heindryckx F, et al. Liver cancer cell lines treated with doxorubicin under normoxia and hypoxia: cell viability and oncologic protein profile. *Cancers (Basel)* 2019;11:1024. [PubMed: 31330834]
116. Liu Z, Tu K, Wang Y, et al. Hypoxia accelerates aggressiveness of hepatocellular carcinoma cells involving oxidative stress, epithelial-mesenchymal transition and non-canonical hedgehog signaling. *Cell Physiol Biochem* 2017;44:1856–68. [PubMed: 29237157]
117. Liang B, Chen S, Li L, et al. Effect of transcatheter intra-arterial therapies on tumor interstitial fluid pressure and its relation to drug penetration in a rabbit liver tumor model. *J Vasc Interv Radiol* 2015;26:1879–86. [PubMed: 26254117]
118. Nahm JH, Rhee H, Kim H, et al. Increased expression of stemness markers and altered tumor stroma in hepatocellular carcinoma under TACE-induced hypoxia: A biopsy and resection matched study. *Oncotarget* 2017;8:99359–71. [PubMed: 29245907]
119. Johnson CG, Sharma KV, Levy EB, et al. Microvascular perfusion changes following transarterial hepatic tumor embolization. *J Vasc Interv Radiol* 2016;27:133–41.e3. [PubMed: 26321051]
120. Levy EB, Gacchina Johnson C, Jacobs G, et al. Direct quantification and comparison of intratumoral hypoxia following transcatheter arterial embolization of VX2 liver tumors with different diameter microspheres. *J Vasc Interv Radiol* 2015;26:1567–73. [PubMed: 26231108]
121. Hong K, Khwaja A, Liapi E, et al. New intra-arterial drug delivery system for the treatment of liver cancer: preclinical assessment in a rabbit model of liver cancer. *Clin Cancer Res* 2006;12:2563–67. [PubMed: 16638866]
122. Zhang S, Huang C, Li Z, et al. Comparison of pharmacokinetics and drug release in tissues after transarterial chemoembolization with doxorubicin using diverse lipiodol emulsions and CalliSpheres Beads in rabbit livers. *Drug Deliv* 2017;24:1011–17. [PubMed: 28660787]
123. Tanaka K, Maeda N, Osuga K, et al. In vivo evaluation of irinotecan-loaded QuadraSphere microspheres for use in chemoembolization of VX2 liver tumors. *J Vasc Interv Radiol* 2014;25:1727–35.e1. [PubMed: 25239839]
124. Teder H, Johansson CJ, d'Argy R, et al. The effect of different dose levels of degradable starch microspheres (Spherex) on the distribution of a cytotoxic drug after regional administration to tumour-bearing rats. *Eur J Cancer* 1995;31:1701–05.
125. Namur J, Wassef M, Pelage JP, et al. Infrared microspectroscopy analysis of ibuprofen release from drug eluting beads in uterine tissue. *J Control Release* 2009;135:198–202. [PubMed: 19367683]
126. Duan XH, Li H, Ren JZ, et al. Hepatic arterial chemoembolization with arsenic trioxide eluting CalliSpheres microspheres versus Lipiodol emulsion: pharmacokinetics and intratumoral concentration in a rabbit liver tumor model. *Cancer Manag Res* 2019;11:9979–88. [PubMed: 32063723]
127. D’Inca H, Namur J, Ghegediban SH, et al. Automated quantification of tumor viability in a rabbit liver tumor model after chemoembolization using infrared imaging. *Am J Pathol* 2015;185:1877–88. [PubMed: 25979795]

128. Kyle AH, Huxham La, Yeoman DM, et al. Limited tissue penetration of taxanes: a mechanism for resistance in solid tumors. *Clin Cancer Res* 2007;13:2804–10. [PubMed: 17473214]
129. Verret V, Bevilacqua C, Schwartz-Cornil I, et al. IL6 and TNF expression in vessels and surrounding tissues after embolization with ibuprofen-loaded beads confirms diffusion of ibuprofen. *Eur J Pharm Sci* 2011;42:489–95. [PubMed: 21329755]
130. Chung JW, Kim H-C. Can CT following chemoembolization with radiopaque drug-eluting beads tell us how much drug we deliver? *Radiology* 2018;289:405–06. [PubMed: 30106342]
131. Thompson JG, van der Sterren W, Bakhtashvili I, et al. Distribution and detection of radiopaque beads after hepatic transarterial embolization in swine: cone-beam CT versus microCT. *J Vasc Interv Radiol* 2018;29:568–74. [PubMed: 29500000]
132. Marin D, Boll DT, Mileto A, et al. State of the art: dual-energy CT of the abdomen. *Radiology* 2014;271:327–42. [PubMed: 24761954]
133. Clark DP, Ghaghada K, Moding EJ, et al. In vivo characterization of tumor vasculature using iodine and gold nanoparticles and dual energy micro-CT. *Phys Med Biol* 2013;58:1683–704. [PubMed: 23422321]
134. Willeminck MJ, Persson M, Pourmorteza A, et al. Photon-counting CT: technical principles and clinical prospects. *Radiology* 2018;289:293–312. [PubMed: 30179101]
135. Symons R, Krauss B, Sahbaee P, et al. Photon-counting CT for simultaneous imaging of multiple contrast agents in the abdomen: An in vivo study. *Medical Physics* 2017;44:5120–27. [PubMed: 28444761]
136. Leng S, Gutjahr R, Ferrero A, et al. Ultra-high spatial resolution multi-energy CT using photon counting detector technology. *Proc SPIE Int Soc Opt Eng*; 2017.
137. de Ruiter Q, Negussie AH, Pritchard WF, et al. Imageability of bismuth radiopaque beads in microCT and clinical dual-energy CT. Society for Interventional Oncology Annual Scientific Meeting. New Orleans, Louisiana 2020.
138. Greten TF, Mauda-Havakuk M, Heinrich B, et al. Combined locoregional-immunotherapy for liver cancer. *J Hepatol* 2019;70:999–1007. [PubMed: 30738077]
139. Duffy AG, Ulahannan SV, Makorova-Rusher O, et al. Tremelimumab in combination with ablation in patients with advanced hepatocellular carcinoma. *J Hepatol* 2017;66:545–51. [PubMed: 27816492] ** Important clinical trial evaluating the combination of tremelimumab, an anti-CTLA-4 checkpoint inhibitor, with ablation or chemoembolization in patients with advanced HCC
140. Lee HW, Cho KJ, Park JY. Current status and future direction of immunotherapy in hepatocellular carcinoma: what do the data suggest? *Immune Netw* 2020;20:e11. [PubMed: 32158599]
141. Osada T, Chong G, Tansik R, et al. The effect of anti-VEGF therapy on immature myeloid cell and dendritic cells in cancer patients. *Cancer Immunol Immunother* 2008;57:1115–24. [PubMed: 18193223]
142. Terme M, Colussi O, Marcheteau E, et al. Modulation of immunity by antiangiogenic molecules in cancer. *Clin Dev Immunol* 2012;2012:492920. [PubMed: 23320019]
143. Huang H, Langenkamp E, Georganaki M, et al. VEGF suppresses T-lymphocyte infiltration in the tumor microenvironment through inhibition of NF- κ B-induced endothelial activation. *FASEB J* 2015;29:227–38. [PubMed: 25361735]
144. Griffioen AW, Damen CA, Blijham GH, et al. Tumor angiogenesis is accompanied by a decreased inflammatory response of tumor-associated endothelium. *Blood* 1996;88:667–73. [PubMed: 8695814]
145. Malo CS, Khadka RH, Ayasoufi K, et al. Immunomodulation mediated by anti-angiogenic therapy improves CD8 T Cell immunity against experimental glioma. *Front Oncol* 2018;8:320. [PubMed: 30211113]
146. de Aguiar RB, de Moraes JZ. Exploring the immunological mechanisms underlying the anti-vascular endothelial growth factor activity in tumors. *Front Immunol* 2019;10:1023. [PubMed: 31156623]
147. Finn RS, Qin S, Ikeda M, et al. Atezolizumab plus Bevacizumab in Unresectable Hepatocellular Carcinoma. *N Engl J Med* 2020;382:1894–905. [PubMed: 32402160]

148. Ager CR, Reilley MJ, Nicholas C, et al. Intratumoral STING activation with T-cell checkpoint modulation generates systemic antitumor immunity. *Cancer Immunol Res* 2017;5:676–84. [PubMed: 28674082]
149. Mullins SR, Vasilakos JP, Deschler K, et al. Intratumoral immunotherapy with TLR7/8 agonist MEDI9197 modulates the tumor microenvironment leading to enhanced activity when combined with other immunotherapies. *J Immunother Cancer* 2019;7:244. [PubMed: 31511088]
150. Kerr WG, Chisholm JD. The next generation of immunotherapy for cancer: small molecules could make big waves. *J Immunol* 2019;202:11–19. [PubMed: 30587569]
151. Ong CJ, Ming-Lum A, Nodwell M, et al. Small-molecule agonists of SHIP1 inhibit the phosphoinositide 3-kinase pathway in hematopoietic cells. *Blood* 2007;110:1942–9. [PubMed: 17502453]
152. Liu Y, Wang X, Deng L, et al. ITK inhibition induced in vitro and in vivo anti-tumor activity through downregulating TCR signaling pathway in malignant T cell lymphoma. *Cancer Cell Int* 2019;19:32. [PubMed: 30814910]
153. Deng J, Li J, Sarde A, et al. Hypoxia-induced VISTA promotes the suppressive function of myeloid-derived suppressor cells in the tumor microenvironment. *Cancer Immunol Res* 2019;7:1079–90. [PubMed: 31088847]
154. Shen L, Qi H, Chen S, et al. Cryoablation combined with transarterial infusion of pembrolizumab (CATAP) for liver metastases of melanoma: an ambispective, proof-of-concept cohort study. *Cancer Immunol Immunother* 2020;69:1713–24. [PubMed: 32333081]
155. Sato T, Eschelmann DJ, Gonsalves CF, et al. Immunoembolization of malignant liver tumors, including uveal melanoma, using granulocyte-macrophage colony-stimulating factor. *J Clin Oncol* 2008;26:5436–42. [PubMed: 18838710]
156. Singh P, Toom S, Avula A, et al. The immune modulation effect of locoregional therapies and its potential synergy with immunotherapy in hepatocellular carcinoma. *J Hepatocell Carcinoma* 2020;7:11–17. [PubMed: 32104669]
157. Sasikumar PG, Ramachandra M. Small-molecule immune checkpoint inhibitors targeting PD-1/PD-L1 and other emerging checkpoint pathways. *BioDrugs* 2018;32:481–97. [PubMed: 30168070]
158. Guzik K, Tomala M, Muszak D, et al. Development of the inhibitors that target the PD-1/PD-L1 interaction—a brief look at progress on small molecules, peptides and macrocycles. *Molecules* 2019;24:2071. [PubMed: 31151293]
159. Boulin M, Guiu S, Chauffert B, et al. Screening of anticancer drugs for chemoembolization of hepatocellular carcinoma. *Anticancer drugs* 2011;22:741–8. [PubMed: 21487286]
160. Fako V, Wang XW. The status of transarterial chemoembolization treatment in the era of precision oncology. *Hepat Oncol* 2017;4:55–63. [PubMed: 28989699]
161. Kumar G, Goldberg SN, Gourevitch S, et al. Targeting STAT3 to suppress systemic pro-oncogenic effects from hepatic radiofrequency ablation. *Radiology* 2017;286:524–36. [PubMed: 28880787]

Article highlights

- Drug-eluting embolic microspheres / beads serve as an embolic agent to stop blood flow to tumors and as a drug delivery vehicle for transarterial chemoembolization (TACE) of hepatic malignancies.
- DEE microspheres increase drug concentrations in tumors and reduce systemic drug exposure compared to conventional drug delivery methods
- Rational selection of drugs for combination with DEE microspheres could exploit potential synergy between mechanisms of drug activity and biologic responses to TACE to enhance efficacy.
- Image-able DEE microspheres may enable “image-guided drug dosimetry” for rational drug targeting of specific drugs to discrete microenvironments within heterogeneous tumors.
- Combinations of DEE microspheres and immune-modulating agents could provide potent local and systemic therapeutic effects by promoting anti-tumor immune responses generated by TACE

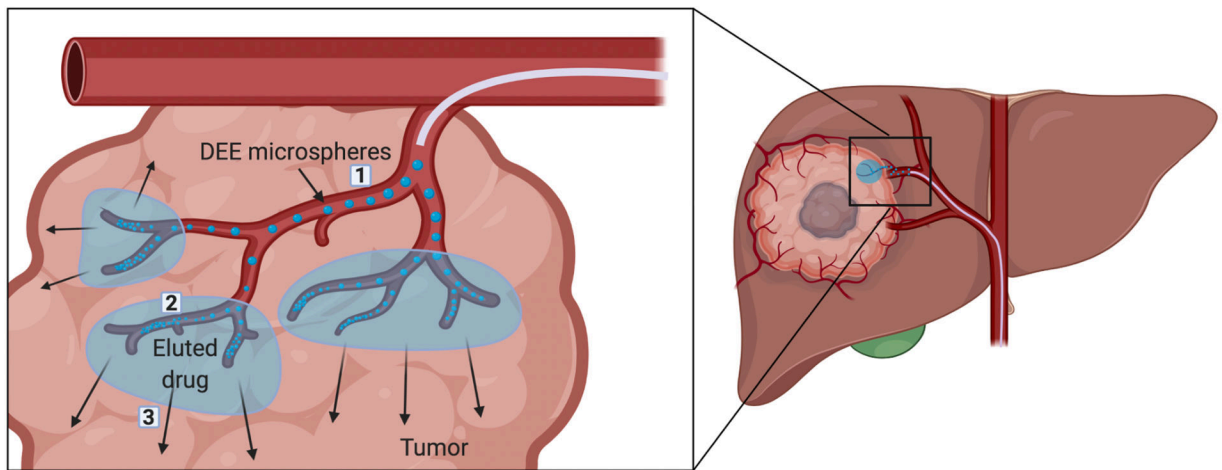


Figure 1.

Schematic representation of theoretical phases of DEE microsphere-based drug delivery, *in vivo*. 1) DEE microspheres are injected via intra-arterial catheter into hepatic arteries supplying the tumor. Drug release is rapid as DEE microspheres are transported with high surface area exposed to flowing blood rich in ions. 2) DEE microspheres become packed in arteries, reducing the overall surface area exposed to blood. Blood flow begins to slow and the rate of drug release diminishes. A blood clot is formed, reducing or eliminating blood flow, and further reducing the rate of drug release. 3) The eluted drug traverses the blood vessel wall and penetrates into the interstitial space primarily by diffusion. Adapted from [107] with permission from Elsevier.

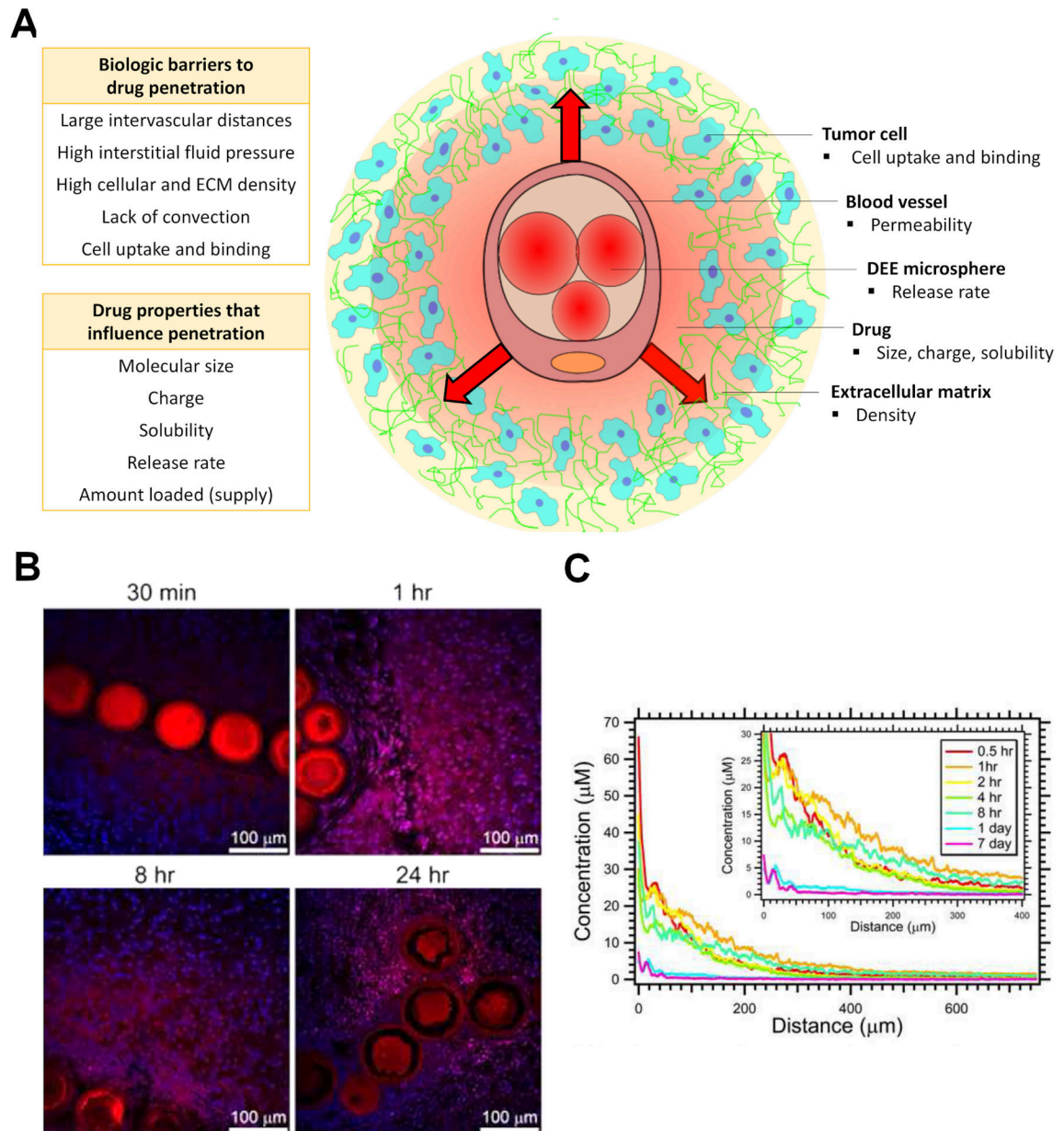


Figure 2.

(A) Factors that may affect drug penetration in tumors after release from DEE microspheres.

(B) Distribution of doxorubicin (red) relative to DEE microspheres and cell nuclei (blue)

over time following TACE in swine liver. C) Doxorubicin concentration versus distance from microspheres in swine liver embolized with 70–150 μm DEE microspheres. B and C reproduced from [95] with permission from Elsevier.

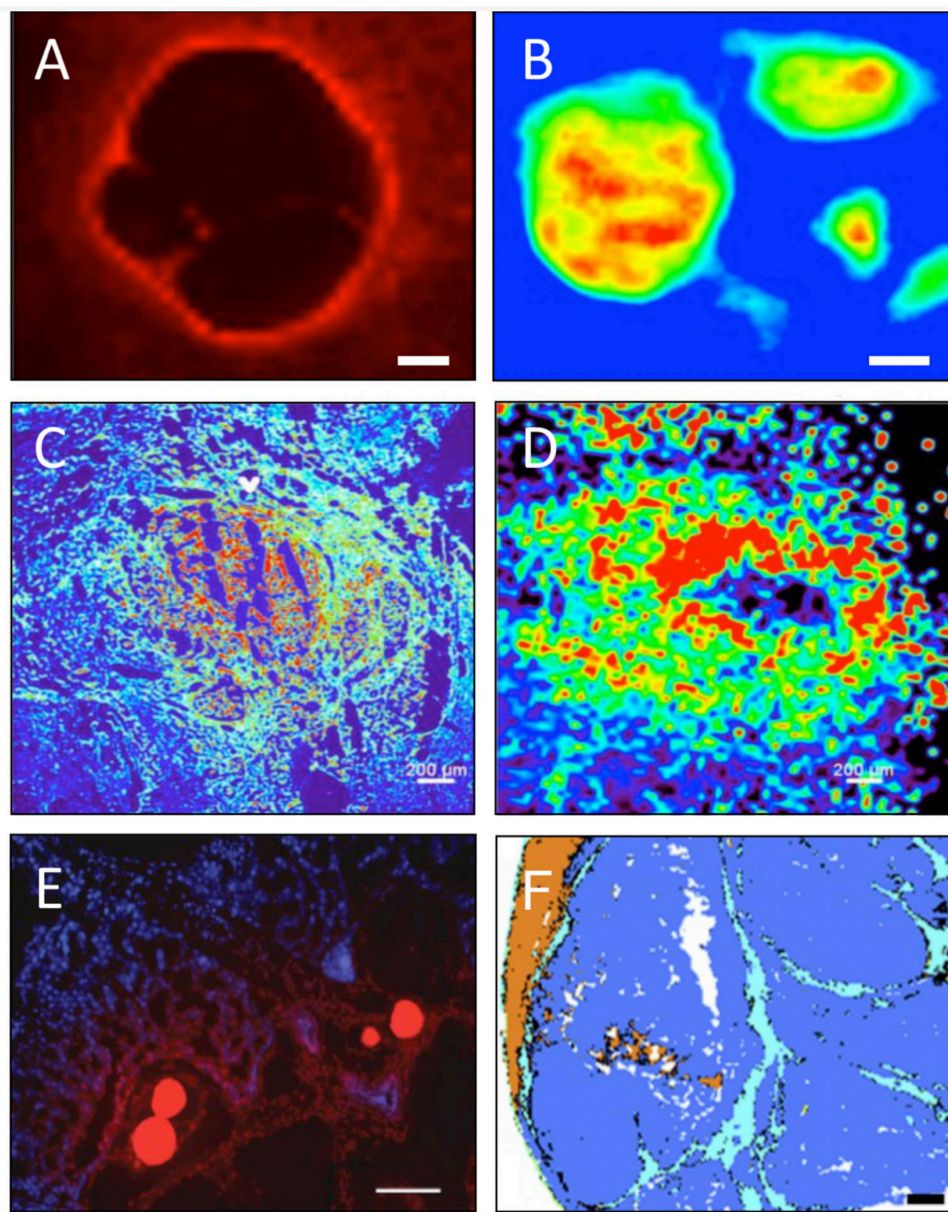


Figure 3. Techniques used to assess drug distribution or treatment effects in tumors after embolization with DEE microspheres. A) Fluorescence microspectroscopy image of eluted doxorubicin surrounding microspheres in a blood vessel (scale bar 50 μm) and B) infrared microspectroscopy demonstrating quantification of doxorubicin inside microspheres, 28 days post-embolization in swine liver (scale bar 70 μm) [103]. C) Fluorescence imaging (pseudo-colored intensity heatmap) and D) mass spectrometry imaging of sunitinib in a tissue section from a rabbit VX2 tumor embolized with sunitinib-eluting microspheres [113]. E) Fluorescence microscopy image of rabbit VX2 tumor section containing doxorubicin-loaded radiopaque microspheres showing doxorubicin (red) *in vivo* elution into tissue (blue cell nuclei) 1 hour after embolization [15]. F) Automated identification of tumor

necrosis (blue), fibrosis (light blue), and liver parenchyma necrosis (brown) using infrared microspectroscopy-based prediction model in a rabbit VX2 tumor section (scale bar 1 mm) [127]. A, B, C, D, and F reproduced with permission from Elsevier. E reproduced with permission from The Radiological Society of North America.

Author Manuscript

Author Manuscript

Author Manuscript

Author Manuscript

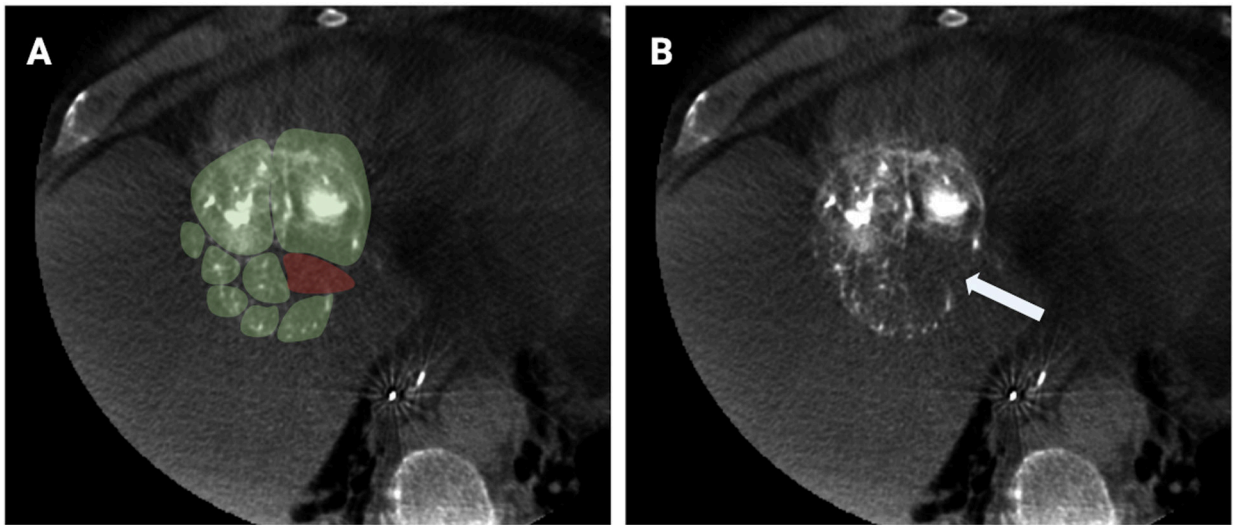


Figure 4. Hypothetical representation of predictive models of spatial drug dosimetry based on radiopaque DEE microsphere attenuation and distribution in an HCC tumor. A) Axial CBCT slice of HCC tumor with green overlay representing hypothetical regions of tumor adequately treated with drug, and red overlay representing potentially undertreated regions. B) CBCT of same tumor showing a paucity of radiopaque DEE microspheres in the region that was illustrated as undertreated. More research is needed to transform this illustration into a method for quantitative prediction of drug distribution and therapeutic effects based on imaged distribution of radiopaque DEE microspheres.

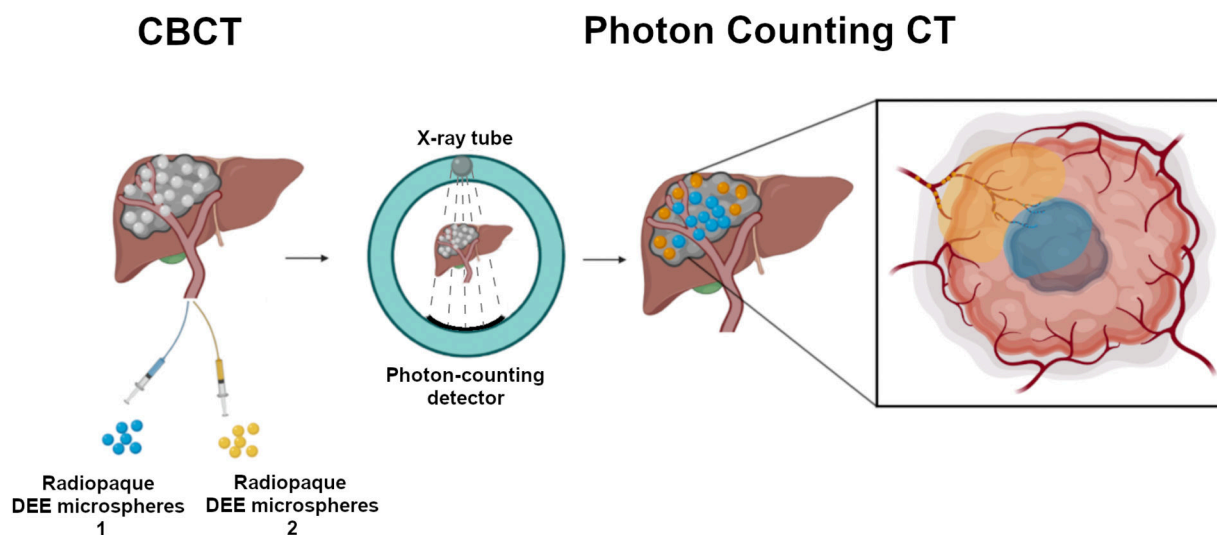


Figure 5.

Concept of “Dual Drug – Dual Microsphere” TACE: delivery of DEE microspheres containing different radiopacifiers and different drugs to specific regions within a tumor, imaged with photon counting CT. Microspheres containing different radiopacifiers and loaded with different drugs are delivered sequentially to different parts of the tumor for rational targeting of discrete intratumoral regions based on drug mechanism of action and expected tumor microenvironment. For example, microspheres with a hypoxia activated drug (blue) may be delivered to hypoxic tumor regions while microspheres with an immune-modulating agent may be directed to immunologically active regions at the tumor margin (yellow). The microspheres cannot be distinguished based on standard unfiltered CBCT (left). Subsequent photon counting CT shows spatial distribution of the two DEE microspheres with different radiopacifiers (center) allowing inferences as to the distribution of the two associated drugs, as shown on the inlay.

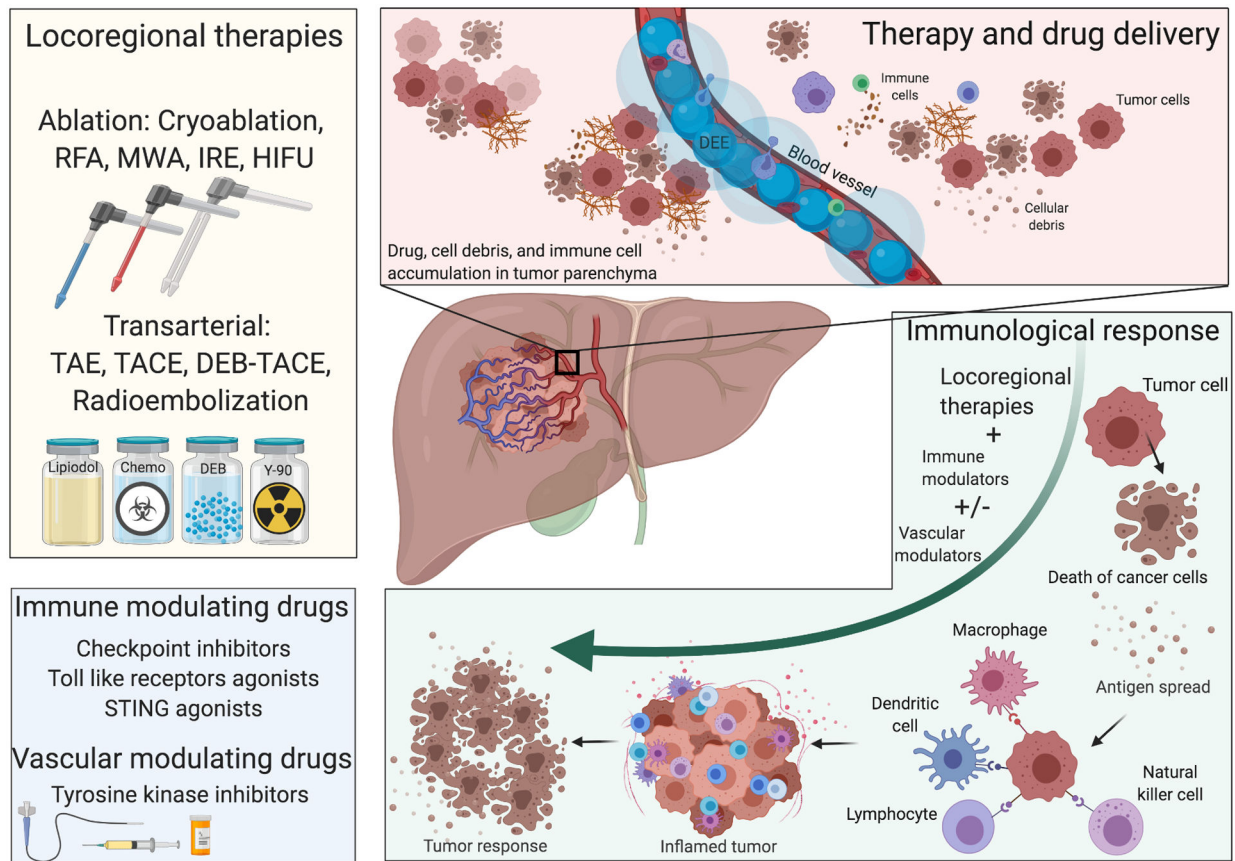


Figure 6.

Immune effects and potential therapeutic strategies using DEE microspheres loaded with immune-modulating agents with or without vascular modulators. Clinically approved drugs as well as novel immune modulators (bottom left) can be delivered in combination with locoregional therapies (top left). This potentially includes TACE in which the immune modulators may be loaded into DEE microspheres as a novel treatment paradigm in HCC. The hypothesis is that intra-arterial delivery of these drugs using DEE microspheres may reduce systemic toxicities, provide greater control over drug spatio-temporal distribution, and promote local immunologic effects initiated by TACE. For example, antigens and cell debris generated by TACE or other locoregional therapies can accumulate in the tumor microenvironment (top right) and trigger a cascade of immunologic events, promoted by immune-modulating agents delivered locally at the site, that include recruitment of immune cells and cytokine release ultimately leading to promotion of antitumor immune responses (bottom right). (RFA: radiofrequency ablation; MWA: microwave ablation; IRE: irreversible electroporation; HIFU: high intensity focused ultrasound; TAE: transarterial embolization)

Table 1.

Characteristics of DEE microspheres and drugs with CE marking, and other drugs that have been loaded.

Commercial Name	Material	Size (µm) [#]	Non-degradable or biodegradable	Examples of drugs loaded	References
DC Bead™ (Boston Scientific, USA)	Polyvinyl alcohol (PVA) cross-linked with 2-acrylamido-2-methyl propane sulfonate	70–150, 100–300, 300–500, 500–700	Non-degradable	doxorubicin [*] , irinotecan [*] , epirubicin, sorafenib, sunitinib, idarubicin, topotecan, mitoxantrone, bevacizumab [§] , rapamycin [‡]	[24–31]
DC Bead LUMI™ (Boston Scientific, USA)	PVA cross-linked with 2-acrylamido-2-methyl propane sulfonate followed by conjugation of iodinated moiety	40–90 (“M0”), 70–150 (“M1”)	Non-degradable	doxorubicin [*] , irinotecan [*] , topotecan, vandetanib	[13, 32–34]
Embozene TANDEM™ (Varian Medical Systems Inc., USA)	Poly(methylmethacrylate) coated with poly(bis(trifluoro-ethoxy)phosphazene)	40±10, 75±15, 100±25	Non-degradable	doxorubicin [*] , irinotecan [*] , idarubicin	[35–37]
HepaSpheres™ (Merit Medical Systems, USA)	Sodium acrylic acid-vinyl alcohol copolymer	30–60, 50–100, 100–150, 150–200	Non-degradable	doxorubicin [*] , irinotecan, epirubicin, idarubicin, oxaliplatin, cisplatin	[37–43]
LifePearl® (Terumo European Interventional Systems, Belgium)	Polyethylene glycol (PEG) and 3-sulfopropyl acrylate	100±25, 200±50, 400±50	Non-degradable	doxorubicin [*] , irinotecan [*] , idarubicin [*] , epirubicin	[37, 44–46]
BioPearl® (Terumo European Interventional Systems, Belgium)	–	–	Biodegradable	doxorubicin [*] , idarubicin [*] , epirubicin	[47]

* Drug CE marked for loading in the corresponding listed DEE microspheres. The remaining drugs are not approved for use with the listed microspheres but their loading has been reported in pre-clinical or clinical investigations. No microspheres are approved for use as drug-eluting devices in the USA.

DC Bead and DC Bead LUMI are cleared for marketing within the US as bland embolic devices.

§ Embozene TANDEM and HepaSpheres are marketed as Embozene™ and QuadraSphere®, respectively, in the US as bland embolic devices.

[#] Size ranges reported by vendor

[§] Loaded using layer-by-layer microsphere coating

[‡] Drug loaded by precipitation within microspheres

[†] Information based on vendor press release

Table 2. Examples of techniques used to measure drug in tumors following TACE with DEE microspheres.

Technique	Examples of drugs measured	Sample preparation	Drug concentration measured in tissue	Drug spatial distribution measured in tissue	Drug measured in microspheres	
LC-MS/MS	Doxorubicin / doxorubicinol, sunitinib, vandetanib, irinotecan (CPT-11, SN38, SN38-G)	Homogenized tissue or biopsy	✓	X	X	[7, 62, 65, 73, 121–123]
LC-FD	Doxorubicin	Homogenized tissue	✓	X	X	[15]
Fluorescence microscopy	Doxorubicin, sunitinib	Tumor section	✓	✓	X	[7, 15, 95, 113]
Autoradiography	¹⁴ C doxorubicin	Whole-body section (rat)	✓	✓	X	[124]
Atomic absorption spectroscopy	Doxorubicin / doxorubicinol	Homogenized tissue	✓	X	X	[102]
Microspectrofluorimetry	Doxorubicin	Tissue section	✓	✓	X	[103, 108, 122]
Infra-red microscopy	Doxorubicin, ibuprofen	Tissue section	X	X	✓	[103, 125]
Mass spectroscopy imaging	Sunitinib and metabolites	Tissue section	✓	✓	X	[113]
Atomic fluorescence	Arsenic trioxide	Homogenized tissue	✓	X	X	[126]